Magnetic Fluctuations in Niobium Pentoxide

Y. Krasnikova, A. A. Murthy, F. Crisa, M. Bal, Z. Sung, J. Lee,
A. Cano, D. M. T. van Zanten, A. Romanenko, and A. Grassellino
Superconducting Quantum Materials and Systems Center (SQMS),
Fermi National Accelerator Laboratory, Batavia, IL 60510, USA

A. Suter, T. Prokscha, and Z. Salman
Laboratory for Muon Spin Spectroscopy, Paul Scherrer Institute, CH-5232 Villigen PSI, Switzerland
(Dated: December 13, 2023)

Using a spin-polarized muon beam we were able to capture magnetic dynamics in an amorphous niobium pentoxide thin film. Muons are working as a probe of this internal magnetic field caused by defects. Magnetic fluctuations could be described by the dynamical Kubo-Toyabe model considering a time-dependent local magnetic field. We state that observed fluctuations result from the correlated motion of electron spins. We expect that oxygen vacancies play a significant role in these films and lead to a complex magnetic field distribution which is non-stationary. The characteristic average rate of magnetic field change is on the order of 100 MHz. The observed dynamics may provide insight into potential noise sources in Nb-based superconducting devices, while also highlighting the limitations imposed by amorphous oxides.

The performance of superconducting qubits is currently limited by a wide variety of loss mechanisms arising from defects and impurities present at material interfaces and surfaces in these devices [1]. It is often a challenge to distinguish between inputs if experimental probe or experimental method itself has a response to many degrees of freedom. Pentoxide in the case of niobium-based qubit devices, the niobium surface oxide that spontaneously grows in ambient conditions serves the major source of microwave loss [2–4]. This loss has been previously linked to the presence of oxygen vacancies [5, 6], as each oxygen vacancy likely introduces an unpaired electron for Nb_2O_5 [7]. Further, antiferromagnetic behavior has been observed in oxygen-deficient niobium oxides [8]. Another one reason why it is worth to take a look on the magnetic footprint in niobium pentoxide is the surface spin model, which was actively discussed for Nb-based SQUID magnetometers [9] and lately for frequency tunable resonators [10]. Oxygen deficiency by itself might cause magnetism, even ferromagnetism in dielectric oxide, when it is not expected [11].

In this Letter, we describe experimental results of low-energy muon spectroscopy as a probe of local magnetism in amorphous niobium pentoxide with various applied magnetic fields and different temperature settings. μSR (muon spin resonance/rotation/relaxation) is a technique that has similarities to both electron spin resonance (ESR) and nuclear magnetic resonance (NMR). It allows for measuring dynamical phenomena occurring on time scales ranging from 10^3 s^{-1} to 10^{12} s^{-1} [12]. The muon lifetime is about 2.2 μs and decaying positrons are emitted along the muon spin direction. As the spin polarization of each muon is impacted by the local magnetic fields present within a solid, the positron counts as a function of time provides insight into the spin depolarization of muons. In these experiments the asymmetry

function, which is directly proportional to the polarization function, is commonly used to describe response to the local magnetic field. The Paul Scherrer Institute has a unique spectrometer operated with a decelerated muon beamline down to keV range. This type of low-energy μSR (LE-μSR) is advantageous as it offers the ability to examine thin film samples. However, in comparison with bulk μSR although beam is quasi-continious, beam deceleration leads to an average of about 1800 events per second. Thus, repeated measurements over several hours required to collect a sufficiently large signal to noise ratio, especially for longitudinal field. Nonetheless, this technique provides unique value in that allows for observing phenomena on time scales that are not accessible with comparable methods such beta-NMR [13], which provides dynamical information from longer time scales. This capability to detect dynamical phenomena across wide range of frequencies combined with the sensitivity to weak magnetic fluctuations makes this technique highly valuable for probing the dynamics at play during superconducting qubit operation.

We have performed LE-μSR studies on amorphous Nb_2O_5 to better understand why this oxide limits the performance of superconducting qubit devices. A thin film of Nb_2O_5 was prepared using DC magnetron sputtering. Microscopy studies show the same amorphous behavior for grown pentoxide film as natively grown pentoxide on top of niobium with the same bonding distances, besides no structural transition appeared during cool down from room temperature down to 4.2 K [14]. This resultant film is found to be amorphous and lack long-range order [14]. X-ray photoelectron spectroscopy (XPS) was used to examine the chemical composition of these films as seen in Fig. 1. From the Nb 3d spectra, we observe that although a majority of the Nb atoms in the oxide layer have a charge state of 5+, which corre-
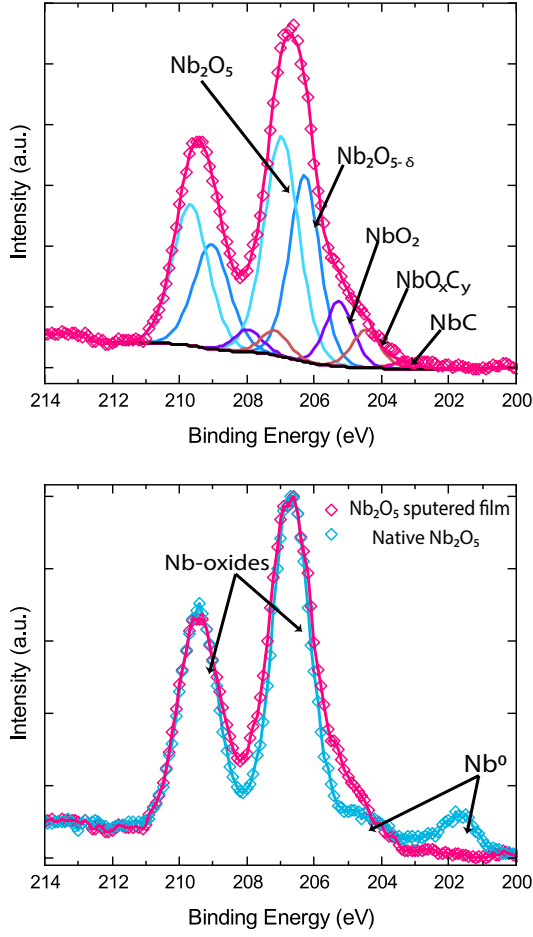
ing time of flight secondary ion mass spectrometry (ToF-SIMS) measurements suggests that the stoichiometry of the Nb_2O_5 thin film sample remains fairly constant. This suggests that the observed oxygen vacancies are dispersed throughout (Supplementary). We do observe the presence of carbon in the top 5nm of Nb_2O_5 thin film, but this signal decays within the film and is attenuated within the depths that we probe with LE muons.

The low-energy muon facility provides the opportunity to vary the beam energy between 1 to 30 keV. In the case of this sample, this roughly corresponds to a range between 10 to 300 nm in thickness, depending on the energy and density of the material. No significant difference was observed for this sample between 3, 9 and 18 keV (20, 55 and 95 nm) [Supplemental materials], which further supports the idea that this film is highly homogeneous. Based on this insight, the mean depth was selected for implanting muons and all further measurements were performed using an average beam penetration depth of $\sim$55 nm (9 keV). By choosing this implantation energy we can be confident that the signal corresponds to dynamical phenomena present in the Nb_2O_5 film as opposed to effects present at the vacuum interface or the substrate.

Two magnetic field configurations were used relative to muon spin. Taking assumption that magnetic field at muon site B_{loc} is homogeneous and parallel to the Z axis The polarization functions could be described as:

$$P_Z(t) = P_Z \exp{(-\lambda_Z t)},$$
$$P_X(t) = P_X \exp{(-\lambda_X t)} \cos(\gamma_\mu B_{loc} t), \qquad (1)$$

λ_X and λ_Z are longitudinal and transverse relaxation rates.

The μSR measurements were taken in zero field (ZF), transverse field (TF) and longitudinal field (LF). The base temperature is 2.8 K. We used musrfit to analyze the μSR data [15].

In case of the transverse field polarization function:

$$P_x(t) = A(T) \exp{(-\lambda t)} \cos(\gamma_\mu B t + \phi), \qquad (2)$$

λ – depolarization rate, $A(T)$ – asymmetry parameter dependent on temperature, γ_μ – muon gyromagnetic ratio, B – magnetic field, ϕ – frequency and phase correspondingly defining muon precession in the magnetic field. The results of fitting are shown in Fig. 2.

In transverse magnetic field, muons start to precess. This precession frequency is defined by external magnetic field. If sample is magnetic, an asymmetry value change will be observed. The asymmetry is plotted as a function of temperature. Based on this plot, we do not observe an obvious footprint associated with a second order transition. However, we observe that magnetic fluctuations appears to be significant below 40 K (Fig. 2). Similarly, the depolarization rate is also temperature-dependent. But the most significant change is observed in the asymmetry, which suggests that there is a finite density of magnetic
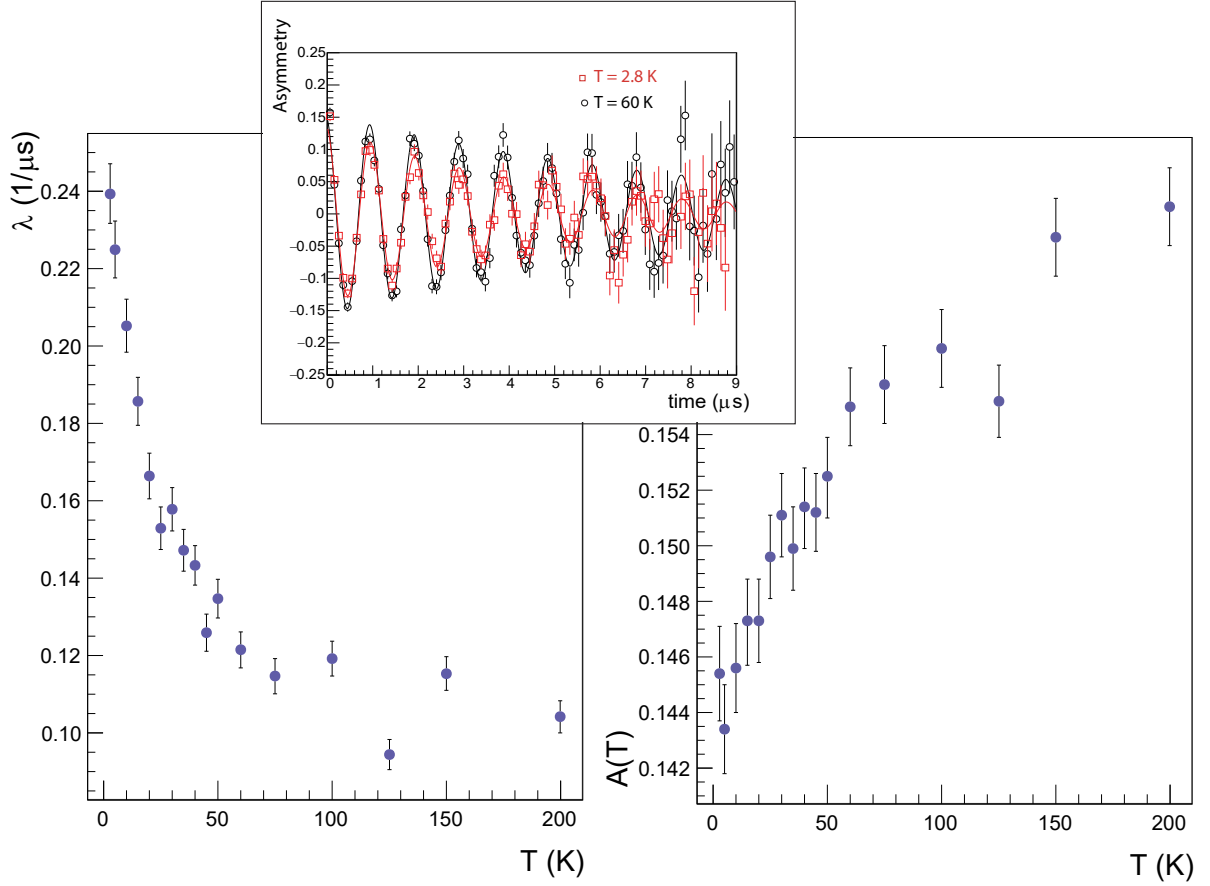

FIG. 1. Upper panel: XPS data analysis for Nb_2O_5 DC sputtered film. Lower panel: XPS data comparison for native surface Nb oxides and Nb_2O_5 DC sputtered film, both are from the same batch as used for measurements at beamfacility at PSI.

sponds to Nb_2O_5, we also observe signal that corresponds to Nb with lower charge states. We attribute this to the presence of oxygen vacancies in the oxide and label the spectral signal as Nb_2O_{5-x}. Nonetheless, through comparison with similar measurements performed at the surface of a Nb film, we observe that the grown Nb_2O_5 film is chemically very similar to the native Nb_2O_5 that forms at the surface of Nb. Namely, we observe alignment in the positions of Nb 3d peaks and a similar broadening in the peaks due to the presence of oxygen vacancies. The Nb0 charge state peak results from photoelectrons that are generated in the Nb that lies beneath surface oxide in the Nb film sample. Further, a depth profile us-

FIG. 2. μSR data in transverse magnetic field 75 Gauss (TF) in Nb_2O_5, $E = 9$ keV. Left panel: temperature dependence of depolarization rate. Right panel: temperature dependence of asymmetry coefficient. Insert: examples of raw data.

centers in the film about non-zero amount of magnetic centers. These centers are capable of depolarizing muons and introducing local magnetic fields, which can be referred to as the internal magnetic field. In the insert for Fig. 2 examples of raw data for captured for two temperatures $T = 2.8$ K and $T = 60$ K is presented. In this case, the amplitude differences are visually distinguishable.

The most common model to describe magnetic fluctuations presence is the dynamical Kubo-Toyabe model [16]. It is a mean-field approximation that takes into account both static and dynamic input in the depolarization function. The rate of fluctuations in this model represents an average rate of collisions (fluctuations). Each muon sitting in the sample will face depolarization due to a stochastically varying field, that is described by multiple "collisions". The hopping rate ν of the model defines time between collisions. For fast fluctuations ($\nu/\Delta >> 1$), there exists an analytical solution [12]. In the case of medium regime, when expansion does not work, an asymmetry function can only be numerically solved. In our case muons are sensitive at rates corresponding to rate

100 MHz, although this can be extended by an order of magnitude to more closely match the operating frequencies of superconducting qubits. Noise sources measured in this regime can potentially serve as sources of decoherence in qubits.

For components of local field:

$$\overline{B_{\mathrm{loc}}(t_0)B_{\mathrm{loc}}(t_0 + t)} = \overline{(B_{\mathrm{loc}})^2}\exp\left(-\nu|t|\right), \quad (3)$$

ν – correlation frequency of the random local field B_{loc}.

Polarization could be defined in case of dynamic input presence by integral equation:

$$P_z(t) = P_z^{\mathrm{stat}}(t)\exp(-\nu t) +$$
$$+\nu\int_0^t P_z(t - t')P_z^{\mathrm{stat}}(t')\exp(-\nu t')dt', \quad (4)$$

In case when $\nu = 0$ polarization is defined by static Kubo-Toyabe function :

$$P_z^{\mathrm{stat}}(t) = A\left(\frac{1}{3} + \frac{2}{3}\exp\left(-1/2\Delta^2 t^2\right)(1 - \Delta^2 t^2)\right), \quad (5)$$
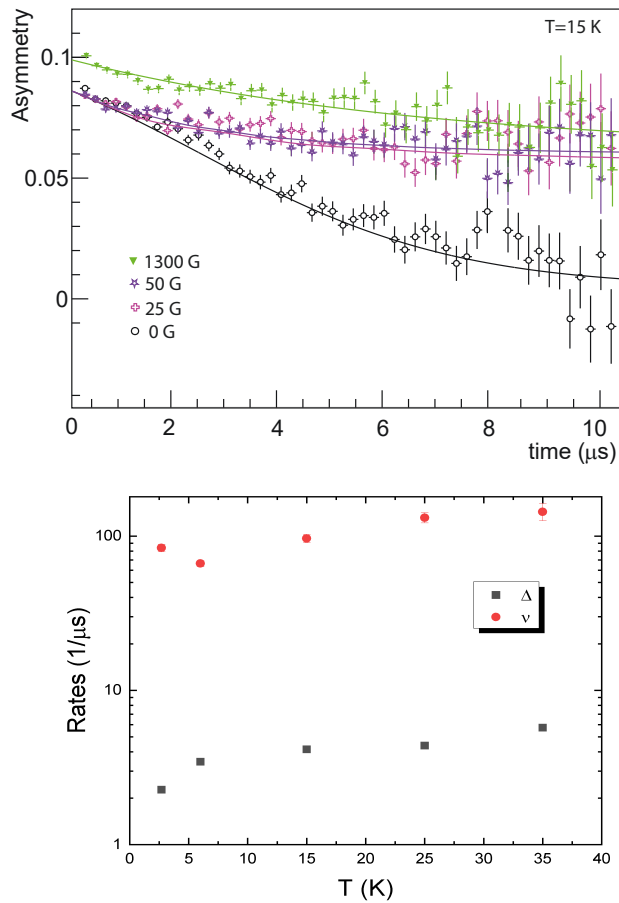
FIG. 4. Naive model to describe polarized muon (μ^+) sitting in complex of vacancies (O_v), nuclear moments are not shown for simplicity. The main assumption that vacancy works as defect and forms trapping potential well, electrons (e) which are sitting inside potential well might have its own spin polarization. This polarization could have time dependent component based on our μSR experimental data, which means that electrons' spins are not frozen.

FIG. 3. μSR data in longitudinal magnetic field (LF) in Nb_2O_5, $E = 9$ keV. Upper panel: Asymmetry function in different magnetic fields at fixed temperature. Lower panel: results of global fitting for asymmetry function at different temperatures, taking dynamic Kubo-Toyabe function, Δ – static and ν – the dynamic rate for local magnetic field.

Δ – static field distribution parameter.

To describe our data, we used a two sub-system approach. We assumed that at high temperatures the asymmetry behavior is largely defined by effects arising from nuclear subsystem, while at lower temperatures we assumed that the asymmetry depends on the sum of both the nuclear and electronic system [14]. The numerical fitting results are shown in Fig. 3.

An important detail of muon spectroscopy is that free unpaired electrons will not depolarize muons. The detected non-zero hopping rate ($\simeq$100 MHz) in dynamical Kubo-Toyabe model is associated with the presence of correlated objects. It is most likely electrons are interacting, potentially forming clusters with non-zero spin and charge density. We are leaving open space for theoreticians to describe flux and charge noise connection for this system. A simplified model of the environment that
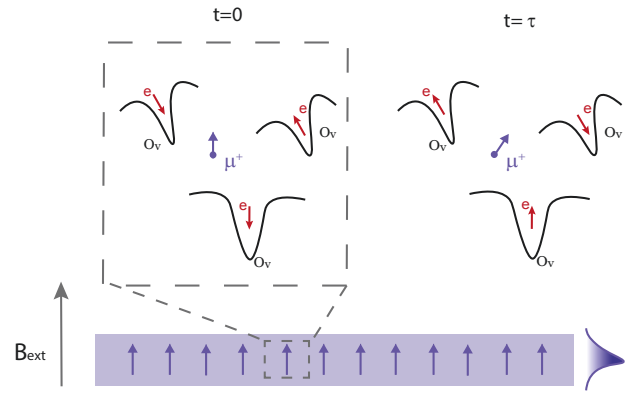
the muon 'sees' local magnetic field in amorphous niobium pentoxide is provided in Fig. 4 and more complex models are necessary to capture the full physics of these interactions. For instance, LF measurements in 1300 G magnetic field still lead to a decrease in the asymmetry, however in this field, nuclear moments are decoupled from muon spin. The drop in asymmetry in this case can be best explained by incorporating the contribution of electrons.

The main conclusion from this study is that electron spins in amorphous niobium pentoxide are not static even in the case where they may be trapped. However, freezing of magnetic moments were not detected at any temperature. Additionally, we observe dynamic depolarization and believe it arises due to electrons. These electrons are not free electrons. Rather, they are correlated, without long-range order formation. The characteristic temperature when these interactions become significant is $T \approx 35$ K (3 meV).

The presence of both dynamic and static magnetic fields in the native surface oxide of niobium could be crucial for superconducting devices due to proximity effect. Static moments may lead to depairing of Cooper pairs and magnetic moments dynamics may contribute to the flux noise.

---

[1] P. Krantz, M. Kjaergaard, F. Yan, T. P. Orlando, S. Gustavsson, and W. D. Oliver, A quantum engineer's guide to superconducting qubits, Applied Physics Reviews **6**, 021318 (2019).

[2] A. Romanenko and D. I. Schuster, Understanding quality factor degradation in superconducting niobium cavities at low microwave field amplitudes, Phys. Rev. Lett. **119**, 264801 (2017).

[3] A. Romanenko, R. Pilipenko, S. Zorzetti, D. Frolov, M. Awida, S. Belomestnykh, S. Posen, and A. Grassellino, Three-dimensional superconducting resonators at $tlt; 20$ mk with photon lifetimes up to $\tau = 2$ s, Phys. Rev. Appl. **13**, 034032 (2020).

[4] M. Bal, A. A. Murthy, S. Zhu, F. Crisa, X. You, Z. Huang, T. Roy, J. Lee, D. van Zanten, R. Pilipenko, I. Nekrashevich, D. Bafia, Y. Krasnikova, C. J. Kopas, E. O. Lachman, D. Miller, J. Y. Mutus, M. J. Reagor, H. Cansizoglu, J. Marshall, D. P. Pappas, K. Vu, K. Yadavalli, J.-S. Oh, L. Zhou, M. J. Kramer, F. Q. Lecocq, D. P. Goronzy, C. G. Torres-Castanedo, G. Pritchard, V. P. Dravid, J. M. Rondinelli, M. J. Bedzyk, M. C. Hersam, J. Zasadzinski, J. Koch, J. A. Sauls, A. Romanenko, and A. Grassellino, Systematic improvements in transmon qubit coherence enabled by niobium surface encapsulation (2023), arXiv:2304.13257 [quant-ph].

[5] E. H. Greener, D. H. Whitmore, and M. E. Fine, Electrical conductivity of near-stoichiometric -nb$_2$o$_5$, The Journal of Chemical Physics **34**, 1017 (1961).

[6] T. Proslier, M. Kharitonov, M. Pellin, J. Zasadzinski, and Ciovati, Evidence of surface paramagnetism in niobium and consequences for the superconducting cavity surface impedance, IEEE Transactions on Applied Superconductivity **21**, 2619 (2011).

[7] P.-D. S. W. Streiff, R., Comment on the defect structure and the transport properties of nb$_2$o$_5$., Oxid Met **3**, 33 (1971).

[8] R. J. Cava, B. Batlogg, J. J. Krajewski, H. F. Poulsen, P. Gammel, W. F. Peck, and L. W. Rupp, Electrical and magnetic properties of nb$_2$o$_{5-\delta}$ crystallographic shear structures, Phys. Rev. B **44**, 6973 (1991).

[9] S. Sendelbach, D. Hover, A. Kittel, M. Mück, J. M. Martinis, and R. McDermott, Magnetism in squids at millikelvin temperatures, Physical review letters **100**, 227006 (2008).

[10] S. E. de Graaf, L. Faoro, L. B. Ioffe, S. Mahashabde, J. J. Burnett, T. Lindström, S. E. Kubatkin, A. V. Danilov, and A. Y. Tzalenchuk, Two-level systems in superconducting quantum devices due to trapped quasiparticles, Science Advances **6**, eabc5055 (2020), https://www.science.org/doi/pdf/10.1126/sciadv.abc5055.

[11] F. C. Venkatesan, M. and J. Coey, Unexpected magnetism in a dielectric oxide., Nature **430**, 630 (2004).

[12] S. J. Blundell, R. De Renzi, T. Lancaster, and F. L. Pratt, 274Low energy μSR, in *Muon Spectroscopy: An Introduction* (Oxford University Press, 2021).

[13] R. Kiefl, G. Morris, P. Amaudruz, R. Baartman, J. Behr, J. Brewer, J. Chakhalian, S. Daviel, J. Doornbos, S. Dunsiger, S. Kreitzman, T. Kuo, C. Levy, R. Miller, M. Olivo, R. Poutissou, G. Wight, and A. Zelenski, Complementarity of low-energy spin polarized radioactive nuclei and muons, Physica B: Condensed Matter **289-290**, 640 (2000).

[14] *Supplemental Materials*.

[15] A. Suter and B. Wojek, Musrfit: a free platform-independent framework for μsr data analysis, Physics Procedia **30**, 69 (2012).

[16] A. Yaouanc and P. Dalmas de Reotier, *Muon spin rotation, relaxation, and resonance: Applications to condensed matter*, Vol. 147 (2011).

[17] M. Wenskat, J. Čižek, M. O. Liedke, M. Butterling, M. Stiehl, G. D. L. Semione, C. Backes, C. Bate, O. Melikhova, E. Hirschmann, A. Wagner, H. Weise, A. Stierle, M. Aeschlimann, and W. Hillert, Vacancy dynamics in niobium and its native oxides and their potential implications for quantum computing and superconducting accelerators, Phys. Rev. B **106**, 094516 (2022).

[18] A. A. Murthy, P. Masih Das, S. M. Ribet, C. Kopas, J. Lee, M. J. Reagor, L. Zhou, M. J. Kramer, M. C. Hersam, M. Checchin, A. Grassellino, R. d. Reis, V. P. Dravid, and A. Romanenko, Developing a chemical and structural understanding of the surface oxide in a niobium superconducting qubit, ACS Nano **16**, 17257 (2022).

Supplemental materials

Film Deposition conditions

Nb_2O_5 films were prepared using sputter deposition. This process involved loading a Si wafer inside an AJA ATC 2200 sputtering system with a base pressure less than 10^{-7} Torr. After dehydrating the substrate under vacuum at 200°C for 30 minutes, the wafer were allowed to cool-down before sputter deposition of Nb_2O_5 at room temperature. DC magnetron sputtering was performed using a 3-inch diameter Nb target with a metals basis purity of 99.95% with an Ar flow rate of 30 sccm, an O_2 flow rate of 20 sccm, and partial pressure of 3.5 mTorr. A sputtering power of 600 W was used and the substrate was rotated at 20 rpm. These conditions resulted in a Nb_2O_5 deposition rate of approximately 5 nm/min.

Film XPS Characterization

X-ray photoelectron spectra were collected using a Thermo Scientific ESCALAB 250Xi XPS spectrometer and a monochromated Al Kα X-ray source with energy 1486.6 eV. The measurement spot size was set to 500 μm and an electron flood gun was used to provide charge compensation. XPS analysis was performed using the Avantage software. All peaks were charged-corrected to the C 1s peak at 284.8 eV. The background signal arising from inelastically scattered electrons was removed using a Shirley baseline model and the peaks were fit using a Gaussian-Lorentzian product.

μSR analysis addendum

TRIM.SP program was used to calculate muon stopping profile. It takes as an input parameter density of material and based on Monte Carlo simulations. For Nb_2O_5 we took 5.2 g/cm^3, it is precise enough for our goals. For energy range up to 15 keV an average penetration depth of muon beam is sitting within 100 nm.
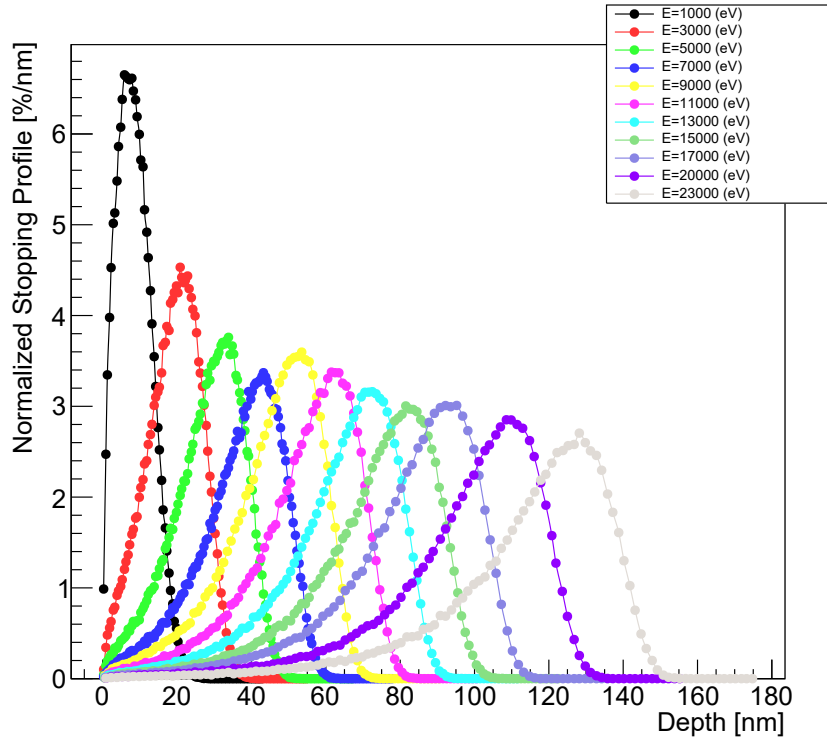

FIG. 1. Simulated muon stopping profile for Nb_2O_5: muons' penetration depth.

Zero field (ZF) muSR doesn't show significant difference for various penetration depth. It confirms that Nb_2O_5 film is uniform, and even more important is uniform from magnetism point of view.

Asymmetry for LF measurements was extracted based on experimental data in the assumption that below 50 K
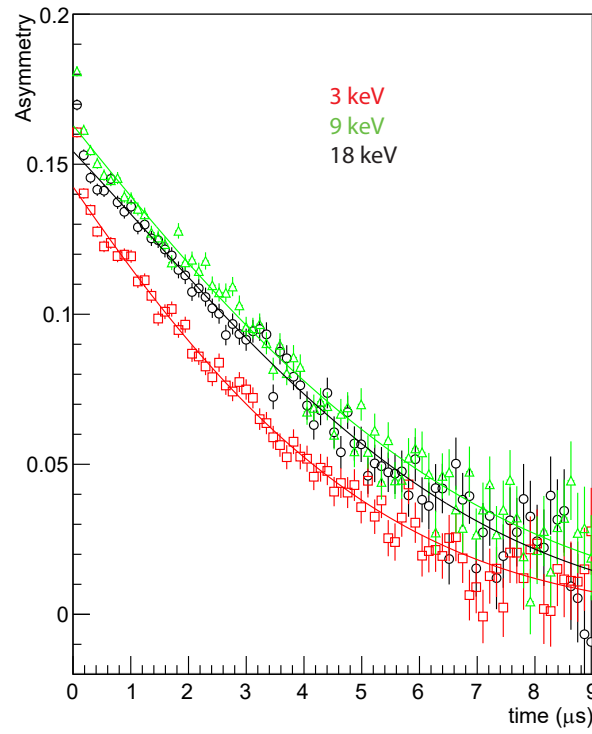
FIG. 2. μSR data in zero magnetic field (ZF) in Nb$_2$O$_5$, for different energies (penetration depths) $E = 3, 9, 18$ keV and base temperature $T = 2.8$ K.

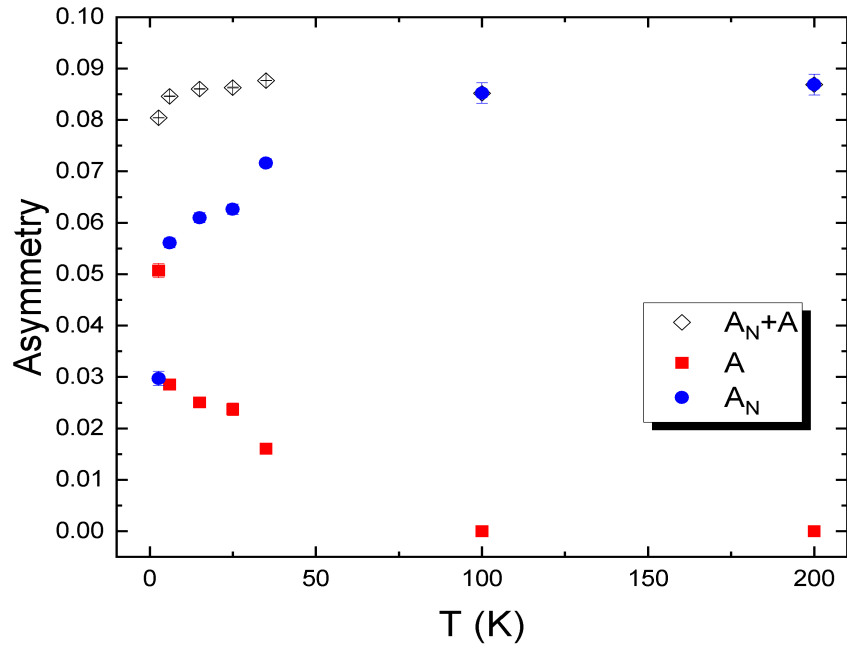FIG. 3. Contributions of nuclear spins (A_N, blue points) and electron spins (A red points) into asymmetry for Nb$_2$O$_5$, sum of inputs shown as black points. All data was obtained from global fit for variety of the longitudinal magnetic field (LF).

temperature electronic system as a contributor to depolarization couldn't be neglected due to high fluctuation rate. Initial fitting took only one system approach and still demonstrated parameter ν significantly non zero in order of tens of MHz. Since applied field was high enough and nucliar system expected to be frozen. Notherless both nuclear and electronic inputs are taken into account during fitting of LF data using dynamical Kubo-Toyabe model. Their asymmetry ratio is representing participation into muons' depolarization. One significant disadvantage that model doesn't take into account interaction between electrons or potential clustering in mean field approach, so fitting doesn't give directly information about number of magnetic centers.